

# Interactions between numerical and experimental approaches in composite structure dynamics

P. Swider<sup>a,\*</sup>, G. Jacquet-Richardet<sup>b</sup>, J. C. Pereira<sup>c</sup>

<sup>a</sup>Laboratoire de Génie Mécanique, Université P. Sabatier Toulouse III, 50 chemin des Maraîchers, 31077 Toulouse cedex 4, France

<sup>b</sup>Laboratoire de Mécanique des Structures ESA CNRS 5006, Bât. 113, INSA Lyon, 20 avenue Albert Einstein, 69621 Villeurbanne cedex, France

<sup>c</sup>Centro Técnico Aeroespacial, Instituto de Aeronautica e Espaço, 1228-904 Sao José dos Campos, SP, Brazil

## Abstract

The objective of this paper is to investigate the interactions linking models and experiments in the dynamics of composite structures. It concerns the validation of predictive models and the characterization of materials. The analysis is supported by the synthesis of four studies and two industrial applications. The numerical models essentially use the finite element method and the experimental modal analysis focuses on natural frequencies, mode shapes, frequency response and damping. In conclusion, certain points of the mixed approach are highlighted and it appears in particular that reciprocation between simulations and tests is frequent and often necessary to improve the efficiency of the design process. © 1998 Elsevier Science Ltd. All rights reserved.

*Keywords:* Composite materials; Dynamics; Modal analysis; Experimental method; Finite element method

## 1. Introduction

The main advantages of composite structures are lightness and anisotropic properties which can be utilized to optimize mechanical behavior. But the increase in stiffness and decrease in mass emphasize vibrating problems, thus the prediction of composite structure dynamic behavior is a very topical subject. Varied fields such as transportation, civil engineering and sports are particularly concerned. Natural frequencies and mode shapes, damping capacities, as well as responses to harmonics, shocks and random excitations are studied.

In this framework, at least two trends of research can be distinguished. The first concerns the development of specific numerical models. The number of works dealing with dynamic problems is rather restricted in dynamics. Certain mechanical problems such as mechanical coupling, warping, transverse shear and damping [1–3] are studied. The second area of research is limited to the loss of reliability of simulation results due to scattering properties: thickness and layer orientations, elastic coefficients, damping

capacities. The dynamic characterization of composite materials has been developed in certain experimental works concerning composite beams and plates with varied geometry and constitutive materials [4,5]. Thus, it appears that a mixed approach, coupling structural modeling to experimentation, is often required to develop reliable dynamic analysis of composite structures.

The main objective of this paper is to highlight interactions between modeling and experimentation in composite structure dynamics. It is based on a synthesis of works involving the validation of predictive models and the dynamic characterization of materials. The numerical models essentially use the finite element method, well adapted to industrial structure calculations, and the structures are composite beams, plates and shells. The experimental modal analysis focuses on natural frequencies, mode shapes, frequency response and damping.

The first analysis concerns the energy balances of transverse shear for multiphase beams. Following this, a specific multilayered shell finite element involving a damping prediction model is presented. Then, the dynamic characterization of the material is reported through the updating of a composite plate and the characterization of a carbon epoxy. Industrial applica-

\*Corresponding author.

tion of the models concerns two applications: part of a car roof and a propfan blade.

## 2. Predictive models

### 2.1. Transverse shear energies for multiphase beams

In the case of multiphase structures, the influence of shear energy is amplified [6,7] and the damping behavior of the structure is dependent on energy distribution. The objective here is to obtain the transverse shear energy balance for multiphase beams with any cross-section in flexion and torsion [8,9]. The shear energy is written in the following form:

$$U_{\tau} = \frac{1}{2} \sum_i \int_{s_i} \left( \frac{\tau_{xy}^2}{G_{xy}} + \frac{\tau_{xz}^2}{G_{xz}} \right) ds_i = \sum_i U_{\tau i} \quad (1)$$

with  $\tau_{xy}$ ,  $\tau_{xz}$  the shear stress in phase  $i$ ;  $G_{xy}$ ,  $G_{xz}$  the shear modulus of phase  $i$ ;  $U_{\tau i}$  the shear energy in phase  $i$ .

The shear stresses are calculated using a finite element resolution of the warping and the stress functions, involving a high precision Hermite element. The direct measurement of strain energy is physically impossible so the validation of the model is carried out by measuring overall quantities. As the torsion loads generate complicated shear stresses, distribution in the cross-section, the center of torsion and the torsion rigidity are measured. The diagram of these set-ups is given in Fig. 1. Rotations of sections ( $\theta$ ,  $\theta_1$ ,  $\theta_2$ ) are measured by inclinometers and the beam is clamped in a torque meter at one end. The punctual force  $P$  is moved horizontally at the free edge of the clamped free beam and the center of rotation position is reached when the inclinometer indicates no rotation. Then the beam is linked by a cylindrical joint at the free end, in order to comply with the free torsion hypothesis, and the torque is

applied around the center of torsion. Torsion stiffness is given by

$$\langle GJ \rangle = \frac{M_x(x_2 - x_1)}{\theta_2 - \theta_1} \quad (2)$$

with  $x_2$ ,  $x_1$  the inclinometer position and  $M_x$  the torsion torque.

The shear energy distribution is sensitive to the geometry of the cross-section (position and shape of the layers) and also to the differential stiffness of the constitutive materials. Symmetrical and non-symmetrical sandwich structures are tested and the constitutive materials were polyurethane-aluminum, wood-epoxy glass. The definition of test profiles is assisted by numerical simulation. The discrepancy between numerical and experimental results concerning the center of torsion position was 2%, while for the torsion stiffness it was 10%. These results are in good agreement considering the materials and profile dispersions. As the torsion stiffness is directly dependent upon shear distribution, the finite element model should give satisfactory shear energy balances.

An industrial application is presented in order to illustrate the interest of this predictive model in a design process. It concerns part of a car roof [9], see Fig. 2. The design parameters are the Young's modulus ( $E_f$ ) and the thickness ( $t_f$ ) of the foam, the Young's modulus of the adhesive ( $E_a$ ) and the thickness of the glass layer ( $t_{gl}$ ). These parameters are modified and the sensitivity analysis concerns the ratio of the modified shear energy  $\Delta U_{\tau}$  versus the reference shear energy  $U_{\tau}$  of the cross-section. The results shown in Fig. 2 highlight the prominent influence of the foam thickness ( $t_f$ ) in flexion and the glass thickness ( $t_{gl}$ ) in torsion. The interest of a validated predictive model appears clearly in this application when seeking increased damping. Experimental studies concerning different roofs have confirmed that when the foam thickness is

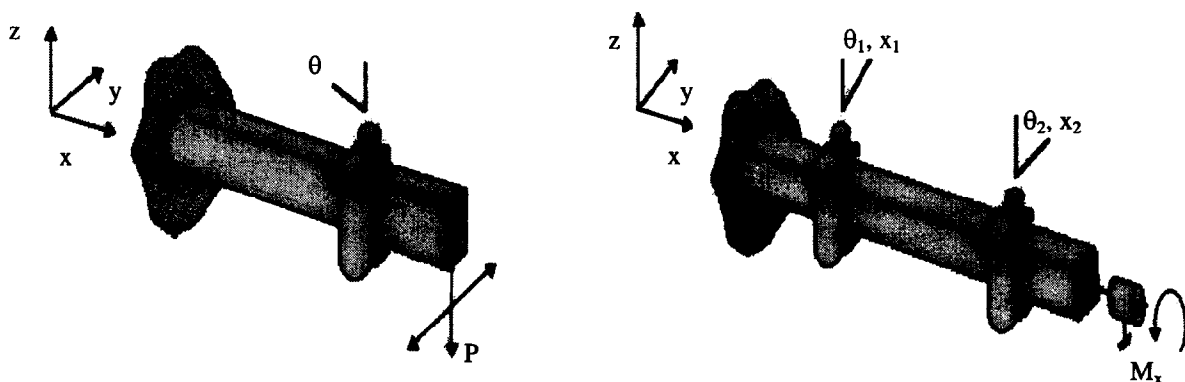
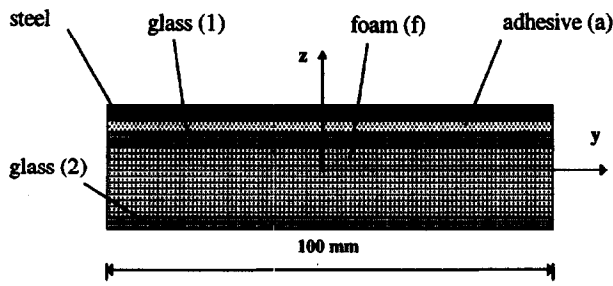


Fig. 1. Torsion test.



	E (Pa)	$\rho$ (kg/m <sup>3</sup> )	$\nu$	t (mm)
steel	2.1e11	7800	0.3	0.8
adhesive (a)	1.0e7	1200	0.48	1.0
glass (g1)	1.0e9	450	0.3	0.8
foam (f)	2.0e6	27	0.4	10.0
glass (g2)	1.0e9	450	0.3	0.6

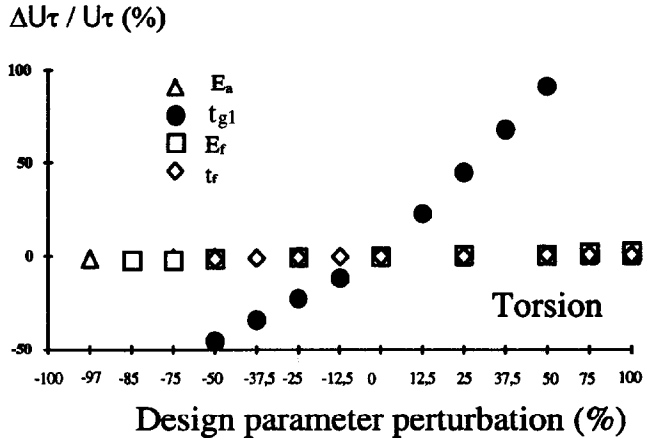
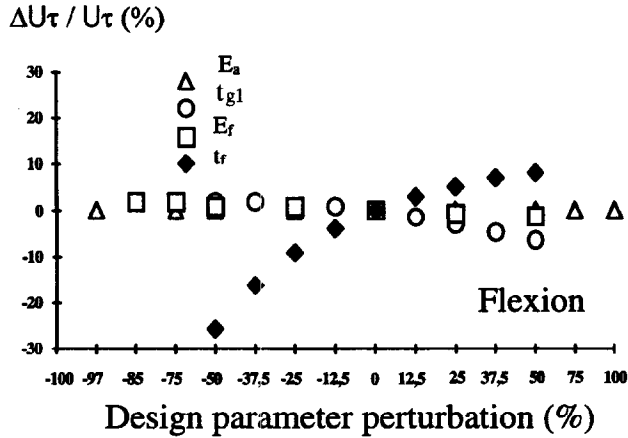


Fig. 2. Part of a car roof.

increased (+50%), damping in flexion increases by about 100%.

2.2. Multilayered shell finite element DQ8

The shell finite element DQ8 [8] is based on the volume breakdown of the shell [10] and the displacement field is assumed to be linear by section along the shell thickness, see Fig. 3. The nodal displacement vector expressed by eqn (3) involves supplementary degrees of freedom  $\alpha_{ik}$ ,  $\beta_{ik}$ , corresponding to layer

rotations. This element is adapted to predict thin and thick shell dynamic behavior involving cross-section warping:

$$\{\delta\}^t = \{u_1, v_1, w_1, \dots, \alpha_8, \beta_8, \dots, \alpha_{1k}, \beta_{1k}, \dots, \alpha_{8k}, \beta_{8k}\} \quad (3)$$

The damping model, first suggested by Adams and Bacon [4], has been completed including coupling terms in the dissipated energy. The material properties are assumed to be linear viscoelastic and the structures are excited by harmonic excitations. The modal damping capacity, eqn (4), involves the specific

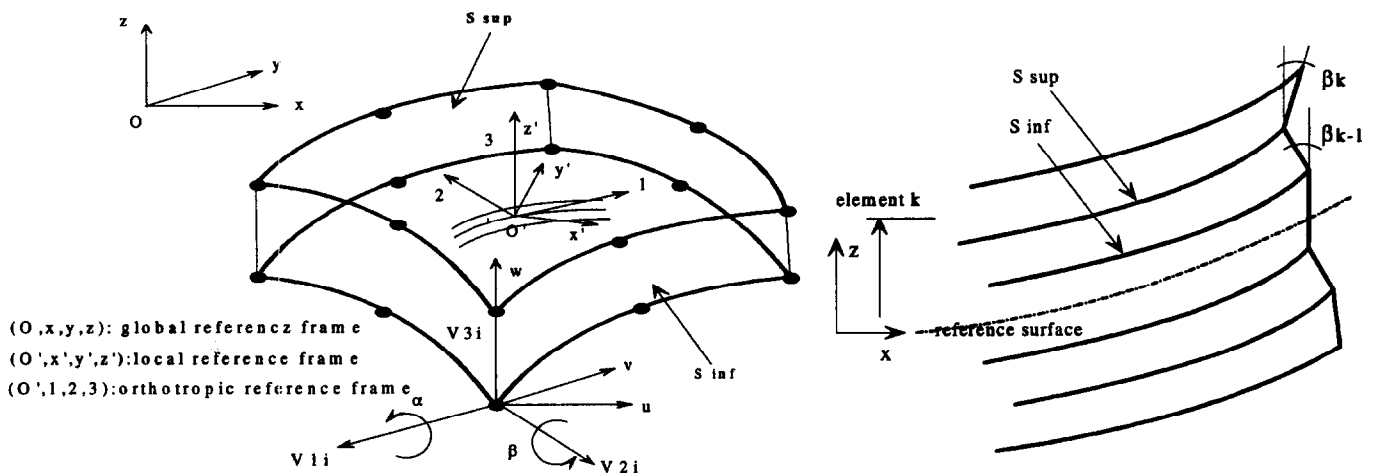


Fig. 3. DQ8 element characterized by a field of linear displacement by section.

damping capacities [8] in  $[Ka]$ . It is linked to the damping factor obtained from the  $-3$  dB bandwidth measurement [11]:

$$\psi_i = \frac{\{\phi_i\}^t \sum_e [Ka]_e \{\phi_i\}}{\{\phi_i\}^t \sum_e [K]_e \{\phi_i\}} = 2\pi\eta_i \quad (4)$$

with  $[Ka]$  the damped stiffness matrix;  $[K]$  the stiffness matrix;  $\{\phi_i\}$  the mode shape;  $\eta_i$  the damping factor ( $-3$  dB bandwidth measurement).

The application considers a clamped-free aluminum shell partially recovered with a sandwich damping device composed of a viscoelastic layer and an aluminum skin, Fig. 4. The most suitable sticking zone corresponds to a common zone of the nodal pattern of the first six modes, where the damping capacity of the viscoelastic layer would be solicited. The dynamic behavior of the structure with and without a damping device is investigated and compared. The frequency response is obtained using white noise excitation in the range 0–500 Hz. The results are given in Table 1. First, the natural frequencies of the isotropic shell are predicted and good agreement with the experimental results is achieved (see Table 1). The discrepancies in the frequencies and the modal damping capacities of the damped shell are less than 7% and 13%, respectively. According to Reissner's model [12], the shear effects are corrected in the composite zone using a global shear factor  $k_g$  or layer by layer shear factors  $k_i$ . The contribution of the covered composite to the total strain energy is low. The slight decrease in frequency induced by the increase in mass is not compensated by an increase in stiffness. This phenomenon, well predicted by the finite element model, involves a somewhat limited sensitivity to shear factors. On the other hand, the viscoelastic material energy and especially the shear energy mostly contribute to the

damping of the whole structure, so the discrete correction is considerable. It has been observed that global correction  $k_g$  might lead to false modal damping capacity values; discrepancies as high as 20% have been obtained.

In conclusion, the progressive correlation between numerical simulation and experimentation has allowed the validation of the finite element, the analysis of specific local phenomena and the testing of the damping model.

### 3. Dynamic characterization of composite materials

#### 3.1. Dynamic updating of a thin carbon epoxy plate

It is generally difficult to control the material and geometrical properties of industrial applications due to manufacturing process scattering. The applications concerns a thin unidirectional carbon epoxy (T300/914) rectangular plate [13], Fig. 5. The updating parameters are the elastic coefficients  $E_1$ ,  $E_2$ ,  $\nu_{12}$ ,  $G_{12}$ ,  $G_{23}$  and ply orientations  $\theta$ . The undamped frequencies obtained from the multilayered shell finite element model presented above are updated using a sensitivity method based on perturbation analysis. Experimental frequencies are used as reference. Starting from the first-order Taylor expansion, the updating parameters  $p_j$  are updated by solving eqn (5)

$$\{\omega_{ei}\} = \{\omega_{ni}\} + [S_{ij}]\{\Delta p_j\} \quad (5)$$

with  $[S_{ij}]$  the sensitivity matrix;  $\omega_{ni}$ ,  $\omega_{ei}$  the numerical and experimental frequencies;  $\Delta p_j$  the updating parameters.

$S_{ij}$  terms are obtained using an order one finite difference formulation. The iterative evaluation of eqn (5) might not converge or might lead to physically

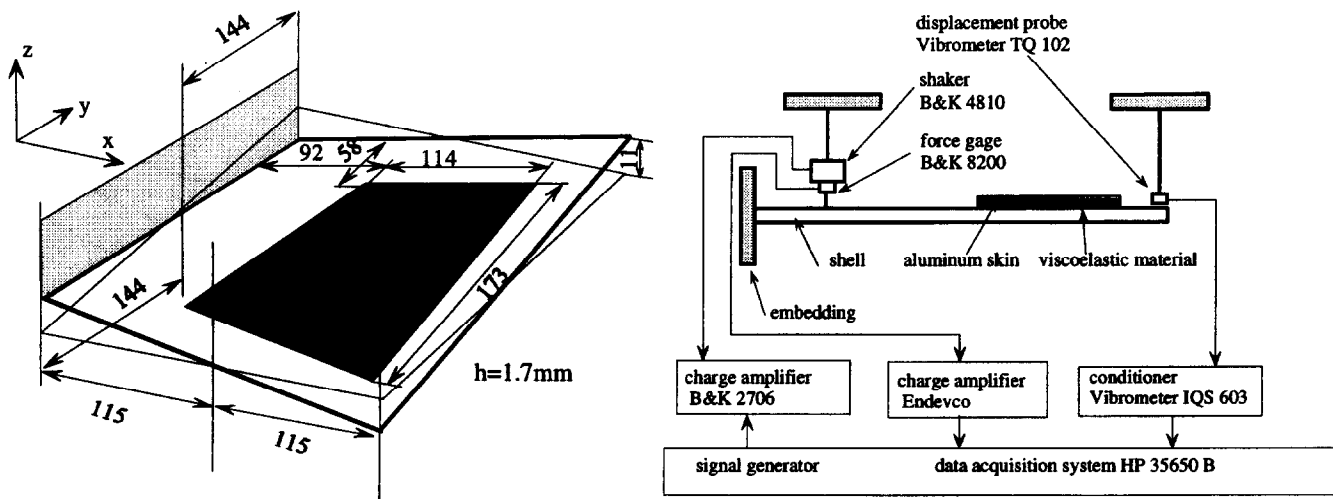
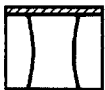
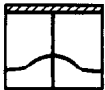


Fig. 4. Clamped-free partially composite twisted shell.

unacceptable values. In order to limit this problem, greater terms of the sensitivity matrix are localized and

the associated equations of eqn (5) are retained. Thus eqn (5) is reduced to its minimum size, as shown in

Table 1  
Composite shell, numerical and experimental results

Mode shape	Isotropic shell			Composite shell			
	$\psi_{exp}$ (%)	$f_{exp}$ (Hz)	$f_{DQ8}$ (Hz)	$\psi_{exp}$ (%)	$\psi_{DQ8}$ (%)	$f_{exp}$ (Hz)	$f_{DQ8}$ (Hz)
	3.6	18.1	28.2 (0.2%)	5.5	5.8 (5.2%)	26.6	26.7 (0.6%)
	1.9	168.3	173.3 (3%)	19.8	17.4 (-12%)	167.3	178.2 (6.5%)
	0.8	205.7	209.8 (2%)	6.2	6.9 (12%)	205.8	212.1 (3.1%)
	0.7	236.2	234.6 (-0.7%)	12.7	12.54 (-1.2%)	233.3	234.4 (0.5%)
	0.9	325.5	334.8 (2.8%)	15.8	13.9 (-12%)	337.6	344.2 (1.9%)
	0.6	431.8	425.7 (-1.4%)	13.8	15.01 (8.6%)	434.9	418.9 (-3.6%)

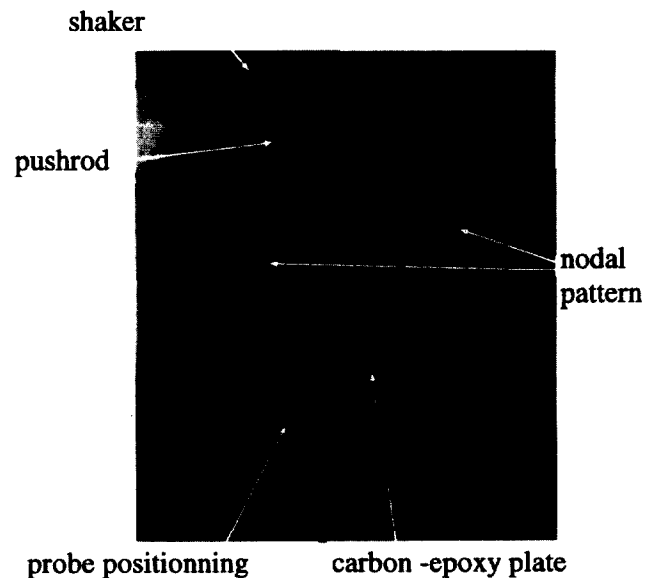
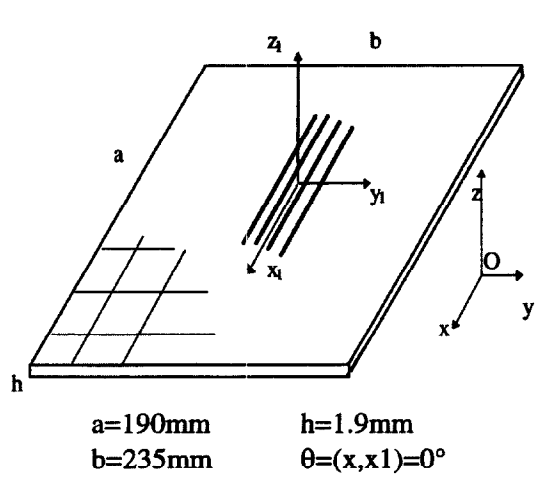


Fig. 5. Carbon epoxy plate.

Table 2. Two different boundary conditions are considered to obtain better uncoupling of the updating parameters. The frequency response of the free plate is obtained using a modal damping model [14]. The frequency and frequency response correlation criteria [15] are defined by eqns (6) and (7), respectively:

$$E_{\omega} = \left[ \sum_i (\omega_{ni} - \omega_{ei})^2 / \sum_i \omega_{ni}^2 \right]^{1/2} \quad (6)$$

$$E_H = \frac{\|H_{ni} - H_{ei}\|}{\|H_{ni}\|} \quad (7)$$

with  $H_{ni}$ ,  $H_{ei}$  the numerical and experimental frequency responses.

After updating, the discrepancies are less than 3% for frequencies and 13% for amplitudes. These results are satisfactory. The observation of sensitivity matrices highlights the coupling of  $E_1$  and  $\theta$ , the complete uncoupling of the influence of  $E_2$  and  $G_{12}$ , and the negligible influence of  $\nu_{12}$  and  $G_{23}$ . In conclusion, this work has permitted updating of the material

properties using a structured analysis of dynamic phenomena.

The mode shapes are very sensitive to the orientation of the plies and boundary conditions. These remarks must be taken into account when the validated models are used as predictive models by development engineers in the composite material industry. This phenomenon is shown in the following shell finite element computation of a NASA SR-3 composite propfan blade [16]. As shown in Fig. 6, the orientation of the plies has been changed by 15°, the variation of frequencies is only 6% and very different mode shapes appear. This phenomenon involves considerable consequential effects for the prediction of the aeroelastic behavior.

### 3.2. Measurement of dynamic elastic coefficients

The scattering of elastic coefficients and damping capacities is rather wide. Furthermore, the static properties of certain materials are different from their dynamic ones due to their viscoelastic behavior. The study is carried out using the experimental natural

Table 2  
Sensitivity matrix

Boundary conditions	Mode shapes	$\delta\omega_{ni}/\delta E_1$	$\delta\omega_{ni}/\delta E_2$	$\delta\omega_{ni}/\delta G_{12}$	$\delta\omega_{ni}/\delta G_{23}$	$\delta\omega_{ni}/\delta \nu_{12}$	$\delta\omega_{ni}/\delta \theta$
F-F-F-F							
	$f_1 = 70 \text{ Hz}$	$7.8 \times 10^{-3}$	$3.7 \times 10^{-2}$	<b>1</b>	$2.5 \times 10^{-3}$	$5.9 \times 10^{-4}$	$-9 \times 10^{-2}$
	$f_2 = 126 \text{ Hz}$	<b>0</b>	<b>1</b>	<b>0</b>	<b>0</b>	<b>0</b>	$-7.5 \times 10^{-3}$
	$f_4 = 292 \text{ Hz}$	<b>1</b>	$3.8 \times 10^{-3}$	<b>0</b>	$5.1 \times 10^{-3}$	$6.4 \times 10^{-3}$	<b><math>8.1 \times 10^{-1}</math></b>
C-F-F-F							
	$f_1 = 24 \text{ Hz}$	$-2.3 \times 10^{-3}$	<b>1</b>	<b>0</b>	<b>0</b>	$4.5 \times 10^{-3}$	$-4.4 \times 10^{-2}$
	$f_3 = 121 \text{ Hz}$	<b>0</b>	<b>1</b>	<b>0</b>	<b>0</b>	$3.7 \times 10^{-3}$	$-2.5 \times 10^{-2}$
	$f_5 = 288 \text{ Hz}$	<b>1</b>	$3.3 \times 10^{-2}$	$4.3 \times 10^{-2}$	$5.4 \times 10^{-3}$	$1.4 \times 10^{-2}$	<b><math>6.1 \times 10^{-1}</math></b>

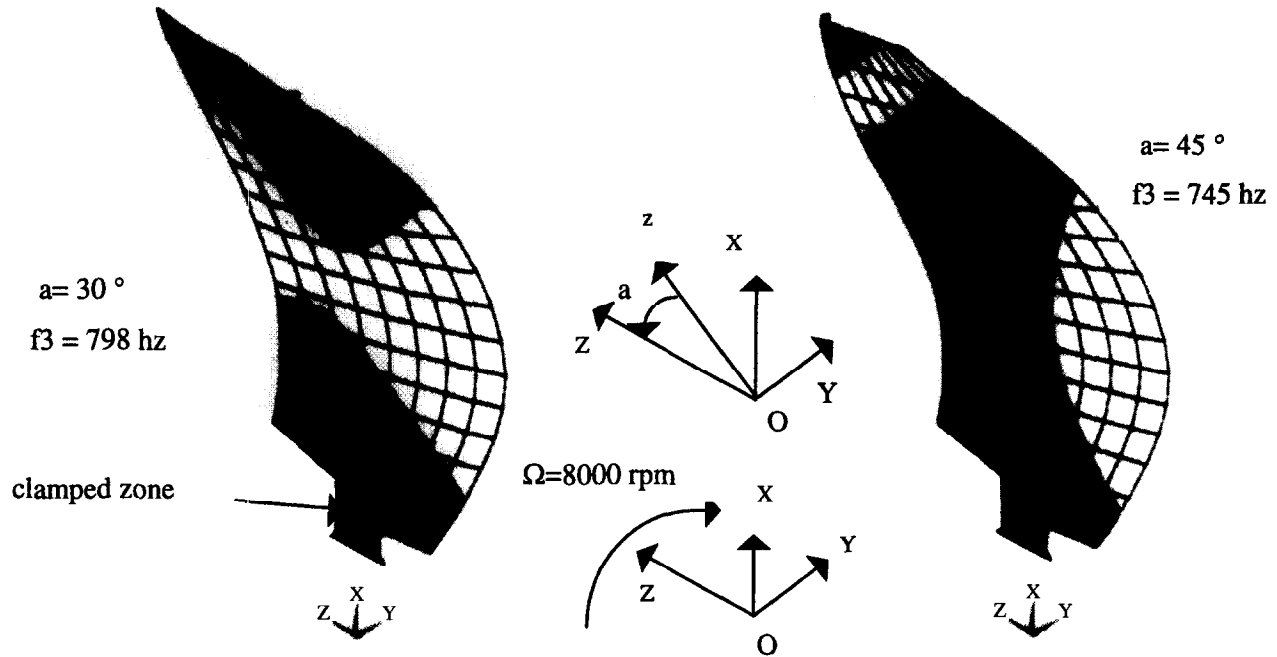


Fig. 6. Propfan blade,  $[90, -a, +a, 90]_s$ , modes 3 and 4,  $a = 30^\circ$  and  $45^\circ$ .

frequencies of a unidirectional carbon epoxy rectangular beam, Fig. 7. Their slenderness ratio is equal to 20 and they are tested in the range 0-500 Hz to limit shear and inertia effects. The experimental stiffnesses are given by analytical relation (8) in flexion and (9) in torsion:

$$\langle EI \rangle = \frac{(4\pi^2 L^4 \rho S f_i^2)}{X_i^2} \quad (8)$$

$$\langle GJ \rangle = \frac{(4\pi^2 L^4 I f_i^2)}{X_i^2} \quad (9)$$

with  $f_i$  the natural frequency;  $X_i$  the dynamic coefficient;  $L$  the beam length;  $S$  the section area;  $\rho$  the density;  $I$  the torsion inertia.

According to the transverse isotropic behavior of the material, coefficients  $E_1$  and  $E_2$  are obtained using eqn (8) for  $0^\circ$  and  $90^\circ$  beams. In torsion, a specific model

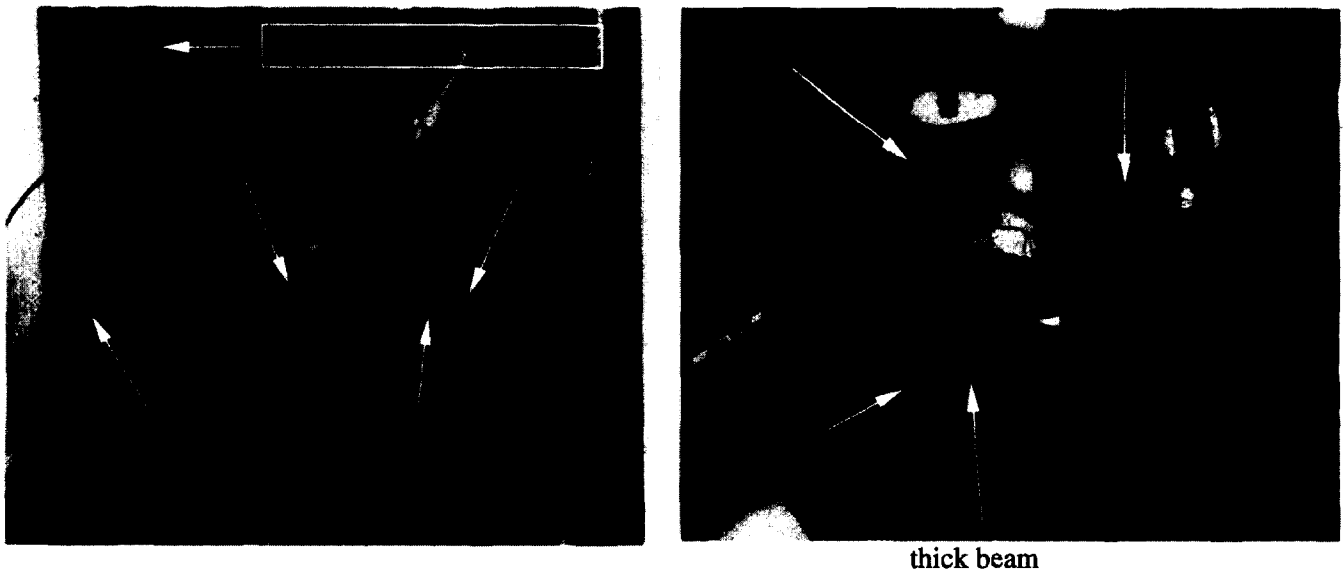


Fig. 7. Characterization of thin and thick carbon epoxy beams.

has been developed based on stress function determination. The approximation of the torsion energy using the Ritz method leads to the torsion stiffness as follows:

$$\langle GJ \rangle = \sum_m \sum_n \frac{256b^3h^3G_{12}G_{13}}{\pi^6m^2n^2(m^2h^2G_{12}+n^2b^2G_{13})} \quad (10)$$

For  $\theta = 0^\circ$ , the transverse isotropy is verified, so eqns (9) and (10) give  $G_{12}$  and  $G_{13}$ . For  $\theta = 90^\circ$ , eqns (9) and (10) give  $G_{23}$ , substituting  $G_{13}$  by  $G_{23}$  due to the rotation of the reference frame. A sensitivity analysis of eqn (10) shows that the sensitivity of  $\langle GJ \rangle$  to  $G_{23}$  decreases when the thickness decreases. Tests carried out on a thick beam with a square cross-section restrict this phenomenon. As the torsion stiffness is high, an inertia disk has been added to reduce torsion frequency, see Fig. 5.

Recent studies [17] have been developed to measure the dynamic Poisson ratio and associated damping capacities using extensometric techniques on unidirectional beams ( $0^\circ$ ,  $90^\circ$ ). At least two perpendicular strain gages ( $i$ ,  $j$ ) are used. The transfer function  $H(j\omega)$ , relation (11), obtained from a spectrum analyser gives the real and imaginary parts of the dynamic Poisson ratio. The associated damping capacities are given by eqn (12):

$$H(j\omega) = \frac{\varepsilon_j(j\omega)}{\varepsilon_i(j\omega)} \quad (11)$$

$$v_{ij}^* = v'_{ij}(1 + j\eta_{ij}) = v'_{ij} \left( 1 + j \frac{\psi_{ij}}{2\pi} \right) = v'_{ij}(1 + j \tan \theta_{ij}) \quad (12)$$

In conclusion, these characterization processes involve important couplings between analytical, semi-analytical developments and experimentation in dynamics.

#### 4. Discussion and conclusion

The synthesis of activities highlights certain important points of a mixed numerical experimental approach for the design of composite structures in dynamics. It appears that if calculations are made before experimentation, design efficiency is improved. Design and production times of experimental devices are decreased, and the models help to analyze the experiment results.

The quality of a model can be checked using calculation–experiment comparison criteria. In statics, the comparative difference between predicted and experimental results is used. It concerns deflection, strain, rupture load value, etc. In dynamics, comparative criteria are not single valued. As shown previously,

they concern natural frequencies (6), dynamic response (7) and mode shapes (Section (A3)3.1). Furthermore, because of their sensitivity to ply orientations and boundary conditions, the correlation of mode shapes is critical in the case of composite structures. The conventional scalar or matricial criteria, such as MAC [15], can be used, but the reliable reconstitution of experimental modes requires many measurements. Field measurement devices well adapted to the experimental modal analysis of composite structures should be used to advantage in the future.

Model updating is achieved using the lowest number of experimental applications, and the analysis of robustness enhances reliability. Numerical and experimental sensitivity analysis provides useful information in order to verify the robustness of the models and the reliability of experimental results. They allow definition of the best adapted tests. The use of statistical techniques is an interesting approach [18]. Generally speaking, the coupling of reliability methods and FEM could be utilized in a judicious manner to predict the dynamic behavior of composite structures [17]. Finally, the utilization of models to predict the dynamic behavior of industrial structures can be achieved within the limits of the family of structures. In the field of composite structures they may be characterized by the constitutive materials, the global geometry and the manufacturing process.

To conclude, it appears that the mixed approach coupling modeling and experimentation is not linear. Reciprocation between simulations and tests is frequent and often necessary. Referring to the optimization concept, the convergence of the process with an ‘objective goal’ should be considered.

#### References

- [1] Chao WC, Reddy JN. Analysis of laminated composite shells using a degenerated 3D element. *Int J Num Meth Eng* 1984;20:1991–2007.
- [2] Saravanos DA. Integrated damping mechanisms for thick composite laminated and plates. *J Appl Mech* 1994;61:375–83.
- [3] Koo KN, Lee I. Vibration and damping analysis of composite laminated using shear deformable finite element. *AIAA J* 1993;31(4):728–35.
- [4] Adams RD, Bacon DGC. Effect of fibre orientation and laminated geometry on the dynamic properties of CFRP. *J Composite Mater* 1973;7:402–28.
- [5] Lin DX, Ni RG, Adams RD. Prediction and measurement of the vibrational damping parameters of carbon and glass fibre-reinforced plastics plates. *J Composite Mater* 1984;18:132–52.
- [6] Nashif AD, Jones DIG, Henderson JP. *Vibration Damping*. New York: Wiley, 1985.
- [7] Ruzika JE, Derby TF, Schubert DW, Pepi JS. Damping of structural composites with viscoelastic shear damping mechanism. *NASA CR 742*, 1967.
- [8] Pereira JC. Contribution a l'étude du comportement mécanique des structures en matériaux composites, caractéristiques

- homogénéisées de poutres composites, comportement dynamique de coques composites. Thèse de Doctorat, INSA Lyon, 1996.
- [9] Pereira JC, Swider P. Bilan des énergies de cisaillement transverse de poutres multiphases isotropes. *Rev Comp Matér Avanc* 1994;4(2):197–211.
- [10] Ahmad S, Irons BM, Zienkiewicz OC. Analysis of thick and thin shell structures by curved finite elements. *Int J Numer Meth Eng* 1970;2:419–51.
- [11] Ewins DJ. *Modal Testing: Theory and Practice*. New York: Wiley, 1984.
- [12] Reissner E. The effect of transverse shear deformations on the bending of elastic plates. *J Appl Mech* 1945;12:A69–77.
- [13] Swider P, Le Fichoux B, Jacquet-Richardet G. Dynamic modelling of a composite plate, a mixed numerical and experimental approach. *Composite Struct* 1996;34:301–08.
- [14] Lalanne M, Berthier P, Der Hagopian J. *Mechanical Vibration for Engineers*. New York: Wiley, 1988.
- [15] Ibrahim SR. Correlation and updating methods: finite element dynamic model and vibration test data. In: *Proceedings of the International Conference on Structure and Dynamics Modelling, Test Analysis and Correlation*. DTA Nafems, 1993.
- [16] Jacquet-Richardet G, Swider P. Influence of fibre orientation on the dynamic behaviour of rotating laminated blades. *Commun Numer Meth Eng*, in press.
- [17] Tranchant C. Modélisation et détermination expérimentale de l'amortissement des structures composites carbone époxyde. *Diplôme d'études approfondies, INSA Lyon*, 1996.
- [18] Béakou A. Méthodes fiabilistes et conception en matériaux composites. *Annal Comp* 1996;1.